

Exclusive heavy quark photoproduction in pp , pPb and $PbPb$ collisions at the LHC and FCC energies

V. P. Gonçalves, G. Sampaio dos Santos, C. R. Sena

High and Medium Energy Group,

Instituto de Física e Matemática,

Universidade Federal de Pelotas

Caixa Postal 354, CEP 96010-900, Pelotas, RS, Brazil

(Dated: March 18, 2022)

In this paper we present a comprehensive analysis of the exclusive heavy quark photoproduction in pp , pPb and $PbPb$ collisions at LHC and FCC energies using the color dipole formalism and taking into account of nonlinear corrections to the QCD dynamics. We estimate the rapidity distributions and cross sections for the charm and bottom production considering three phenomenological models for the dipole-proton scattering amplitude that are able to describe the ep HERA data. Our results indicate that a future experimental analysis of this process is feasible, which will allow us to improve our understanding of the QCD dynamics.

PACS numbers: 12.38.-t; 13.60.Le; 13.60.Hb

Keywords: Ultraperipheral Heavy Ion Collisions, Heavy Quark Production, QCD dynamics

I. INTRODUCTION

One of the main goals of Particle Physics is to achieve a deeper knowledge of the hadronic structure. A multidimensional partonic imaging of the hadron is provided by the 5-dimensional QCD Wigner distributions, which encode all quantum information about partons, including information on both generalized parton distributions (GPD) and transverse momentum dependent parton distributions (TMD) (See, e.g Refs. [1–4]). In the last years several authors proposed to constrain the gluon Wigner distribution in the nucleon by studying different final states that can be generated in photon-induced interactions present in electron-hadron and hadron-hadron collisions [5–13]. One of the more promising processes is the exclusive dijet photoproduction in ultraperipheral hadronic collisions [7], which are characterized by an impact parameter that is larger than the sum of the radius of the incident hadrons [14]. In such collisions the final state is very clean, being characterized by the dijet, two intact hadrons and two rapidity gaps associated to the photon and Pomeron exchanges. However, the measurement of the angular distribution of the Wigner distribution in this final state is challenging, since it requires reconstruction of full dijet kinematics. An alternative is to consider the exclusive heavy quark photoproduction in hadronic collisions [12]. As demonstrated for the first time in Ref. [15], such process probes the nonlinear corrections to the QCD dynamics at high energies [16]. In order to reconstruct the isotropic and elliptic components of the gluon Wigner distribution, it is fundamental to access the dependence of the differential distribution in the relative quark-antiquark momentum for distinct values of the momentum transfer. Such analysis will only be feasible if the corresponding number of events generated in the current and/or future colliders is large. The main goal of this paper is to estimate the cross sections for the exclusive charm and bottom photoproduction in pp , pPb and $PbPb$ collisions using the Color Glass Condensate formalism [17]. In our study we will consider two very successful implementations of this formalism, the bCGC and IP-SAT models, which are able to describe the inclusive and exclusive ep HERA data. For comparison, predictions derived using the IPnonSAT model, which disregards the nonlinear effects, will also be presented. We will derive predictions for the rapidity distributions and cross sections for the LHC energies, which update the results presented in Ref. [15]. Moreover, predictions for the center-of-mass energies of the Future Circular Collider (FCC) [18] will be presented for the first time. Finally, a comparison between the predictions for the exclusive and inclusive heavy quark photoproduction will also be presented. As we will demonstrate below, our results indicate that a future experimental analysis of the exclusive heavy quark photoproduction is feasible and that this process can be used to improve our understanding of the QCD dynamics. In addition, the large number of events expected for the LHC and FCC, in particular for charm production, will allow to study more differential distributions, as those necessary to constrain the elliptic component of the gluon Wigner function.

The paper is organized as follows. In Sec. II we present a brief review of the color dipole formalism and the main expressions used to estimate the exclusive heavy quark photoproduction. Moreover, the distinct models for the dipole – hadron scattering amplitude are discussed. In Sec. III, we present our predictions for the cross sections and rapidity distributions to be measured in $pp/pPb/PbPb$ collisions at the LHC and FCC energies. Finally, in Sec. IV, we summarize our main conclusions.

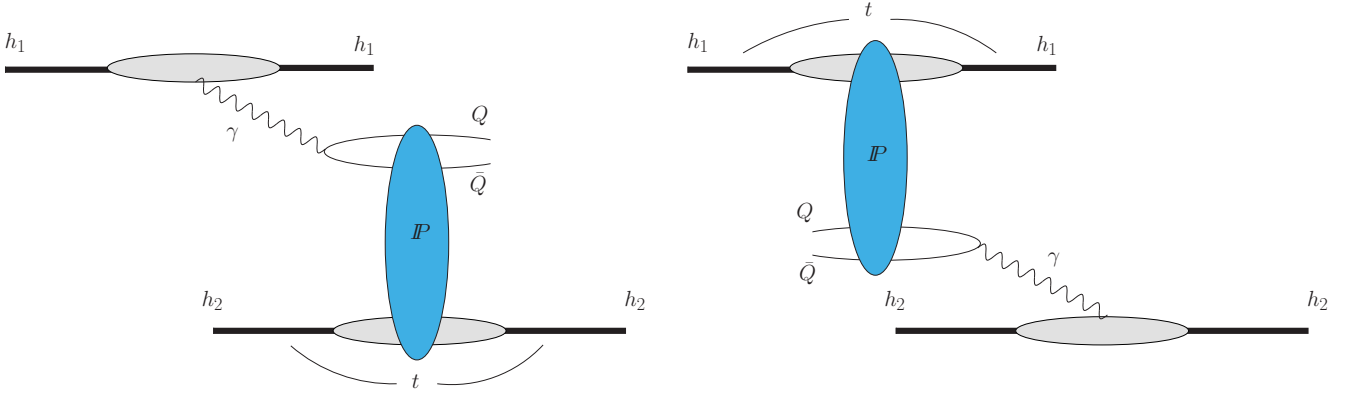


FIG. 1: Typical diagrams for the exclusive heavy quark photoproduction in a hadronic collision.

II. FORMALISM

The typical diagrams for the heavy quark production in ultraperipheral collisions (UPC), where the photon-induced interactions are dominant, are represented in Fig. 1. The hadrons act as a source of almost real photons and the hadron-hadron cross section for the exclusive heavy quark photoproduction can be written in a factorized form, described using the equivalent photon approximation [14]. In the color dipole formalism [20], the γh interaction can be expressed in terms of a (color) dipole-hadron interaction and the nonlinear effects in the QCD dynamics [16] can be taken into account. In this formalism, the photon-hadron cross section for the exclusive heavy quark production is given by

$$\sigma_{\gamma h \rightarrow Q\bar{Q}h}(W_{\gamma h}) = \frac{1}{4} \int dz d^2\mathbf{r} |\Psi^T(z, \mathbf{r})|^2 \int d^2\mathbf{b}_h \left(\frac{d\sigma}{d^2\mathbf{b}_h} \right)^2, \quad (1)$$

where $W_{\gamma h}$ is the photon – hadron center – of – mass energy, z is the photon momentum fraction carried by the quark, \mathbf{r} is the transverse dipole separation and \mathbf{b}_h is the impact parameter, given by the transverse distance between the centers of the dipole and the target. Moreover, for a transversely polarized photon with $Q^2 = 0$ one has that the squared wave function $|\Psi^T(z, \mathbf{r})|^2$ is given by [20]

$$|\Psi^T(z, \mathbf{r})|^2 = \frac{6\alpha_{em} e_Q^2}{(2\pi)^2} \{m_Q^2 K_0^2(m_Q r) + m_Q^2 [z^2 + (1-z)^2] K_1^2(m_Q r)\}, \quad (2)$$

where α_{em} is the electromagnetic coupling constant, e_Q is the fractional quark charge and m_Q the mass of the heavy quark. Furthermore, $x = 4m_Q^2/W_{\gamma h}^2$ and the differential dipole-hadron cross section can be expressed by

$$\frac{d\sigma}{d^2\mathbf{b}_h} = 2\mathcal{N}_h(x, \mathbf{r}, \mathbf{b}_h), \quad (3)$$

where $\mathcal{N}_h(x, \mathbf{r}, \mathbf{b}_h)$ is the forward dipole-hadron scattering amplitude, which is dependent on the modelling of the QCD dynamics at high energies. As in our previous study [21], we will consider the bCGC [22] and IP-SAT [23] models for the description of the dipole-proton scattering. Although these models differ in the treatment of the impact parameter dependence and/or of the linear and nonlinear regimes, both describe quite well the high precision HERA data. One has that in the bCGC model, the linear regime of the dipole-proton scattering amplitude is described by the solution of the BFKL dynamics near of the saturation line, which implies that $\mathcal{N}_p \propto \mathbf{r}^{2\gamma_{eff}}$ with $\gamma_{eff} \leq 1$. In contrast, the IP-SAT model predicts $\mathcal{N}_p \propto \mathbf{r}^2 xg(x, 4/r^2)$ in the linear regime, where xg is the gluon distribution of the target. On the other hand, the saturation regime is described in the bCGC model by the Levin-Tuchin law [24], while the IP-SAT predicts the saturation of \mathcal{N}_p at high energies and/or large dipoles, but the approach to this regime is not described by the Levin-Tuchin law. In our analysis we will assume for the bCGC model the set of parameters obtained in Ref. [25] by fitting the HERA data on the reduced ep cross sections. For the IP-SAT, we will assume the parameters obtained in Ref. [26]. In addition, we will also present the predictions derived using the IPnonSAT model proposed in Ref. [26], which is obtained disregarding the nonlinear corrections in the IP-SAT model. The comparison between the IP-SAT

and IPnonSAT predictions will allow us to estimate the impact of the nonlinear corrections in the exclusive heavy quark photoproduction in hadronic collisions. For a nuclear target, we will assume that the dipole-nucleus scattering amplitude is given by the model proposed in Ref. [27], which is based on the Glauber-Gribov approach [28–30], being expressed by

$$\mathcal{N}_A(x, \mathbf{r}, \mathbf{b}_A) = 1 - \exp \left[-\frac{1}{2} \sigma_{dp}(x, r^2) T_A(\mathbf{b}_A) \right], \quad (4)$$

where

$$\sigma_{dp}(x, r^2) = 2 \int d^2 \mathbf{b}_p \mathcal{N}_p(x, \mathbf{r}, \mathbf{b}_p), \quad (5)$$

and $T_A(b_A)$ is the nuclear thickness function which is typically obtained from the Woods-Saxon distribution for the nuclear density normalized to the atomic mass A , and b_A is the impact parameter of the dipole with respect to the nucleus center. Although such model describes the scarce existing experimental data on the nuclear structure function [31], future data from the Electron – Ion Collider will be useful to constrain the description of the dipole – nucleus scattering amplitude [3]. We will compute \mathcal{N}_A considering the bCGC, IP-SAT and IPnonSAT models for the dipole-proton scattering amplitude discussed before (For more details see e.g. Ref. [21]).

III. RESULTS

In what follows we will present our predictions for the rapidity distribution and cross sections for the exclusive charm and bottom photoproduction in $pp/pPb/PbPb$ collisions at the LHC and FCC energies. One has that the differential cross section for the exclusive production of a heavy quark $Q\bar{Q}$ at rapidity Y is given by

$$\frac{d\sigma [h_1 + h_2 \rightarrow h_1 + Q\bar{Q} + h_2]}{dY} = [n_{h_1}(\omega) \sigma_{\gamma h_2 \rightarrow Q\bar{Q} h_2} (W_{\gamma h_2}^2)]_{\omega_L} + [n_{h_2}(\omega) \sigma_{\gamma h_1 \rightarrow Q\bar{Q} h_1} (W_{\gamma h_1}^2)]_{\omega_R}, \quad (6)$$

where $\omega_L (\propto e^{+Y})$ and $\omega_R (\propto e^{-Y})$ denote photons from the h_1 and h_2 hadrons, respectively. The center-of-mass energy for the photon-hadron interactions is given by $W_{\gamma h} = \sqrt{4\omega E}$, where $E = \sqrt{s}/2$ and \sqrt{s} is the hadron-hadron center – of – mass energy. Moreover, $n(\omega)$ is the equivalent photon spectrum generated by the hadronic source, which we will assume to be described by the Drees-Zeppenfeld [19] and the relativistic point-like charge [14] models for the case of a proton and a nucleus, respectively. The maximum photon energy can be derived considering that the maximum possible momentum in the longitudinal direction is modified by the Lorentz factor, γ_L , due to the Lorentz contraction of the hadrons in that direction [14]. It implies $\omega_{\max} \approx \gamma_L/R_h$ and, consequently, $W_{\gamma h}^{\max} = \sqrt{2\omega_{\max} \sqrt{s}}$. For the LHC, the maximum photon – nucleon center – of – mass energy, $W_{\gamma h}^{\max}$, reached in $pp/pPb/PbPb$ collisions at $\sqrt{s} = 14/8.1/5.5$ TeV is 8.4/1.4/0.95 TeV [14]. On the other hand, for the FCC we will reach $W_{\gamma h}^{\max} \approx 55/8.7/6.8$ TeV for $pp/pPb/PbPb$ collisions at $\sqrt{s} = 100/63/39$ TeV. Therefore, LHC and FCC probe a range of photon – hadron center – of – mass energies unexplored by HERA. In our calculations, we will assume $m_c = 1.27$ GeV and $m_b = 4.5$ GeV and the phenomenological dipole-proton models discussed above, which describe the ep HERA data, will be considered. The comparison between the IP-SAT, IPnonSAT and bCGC predictions will allow us to estimate the impact of the nonlinear effects, as well of the different descriptions of the transition between the linear and nonlinear regimes. In our analysis, we will assume that the events can be separated with a small experimental uncertainty, associated to e.g. the efficiency of charm and bottom tagging. Surely such aspect deserves a more detailed study in the future.

In Fig. 2 we present the IP-SAT and bCGC predictions for the rapidity distribution considering the exclusive charm and bottom photoproduction in pp collisions at the FCC ($\sqrt{s} = 100$ TeV). The contribution of both terms of Eq. (6) are presented, as well as the sum of them is represented by the solid lines. The first term in Eq. (6), denoted “Left” in the figures, is determined by the photon flux for a photon with a energy $\omega \propto e^Y$ and the exclusive heavy quark photoproduction cross section for a given photon – proton center – of – mass energy $W_{\gamma p}$. While $\sigma_{\gamma p \rightarrow Q\bar{Q} p}$ increases with $W_{\gamma p}$, the photon flux strongly decreases when the photon energy is of the order of $\omega_{\max} \approx \gamma_L/R_p$, becoming almost zero for larger photon energies. As a consequence, this contribution increases with the rapidity up to a maximum and becomes zero at very large Y . On the other hand, the second term in Eq. (6), denoted “Right” in the figures, increases for negative values of rapidity, since in this case $\omega \propto e^{-Y}$. For pp collisions, the contributions of both terms are identical and symmetric in rapidity. Such behaviours are verified in Fig. 2. The increasing with rapidity is determined by the energy dependence of the exclusive heavy quark photoproduction cross section, being dependent on the dipole model considered. For the bottom production, the IP-SAT model predicts a faster increasing

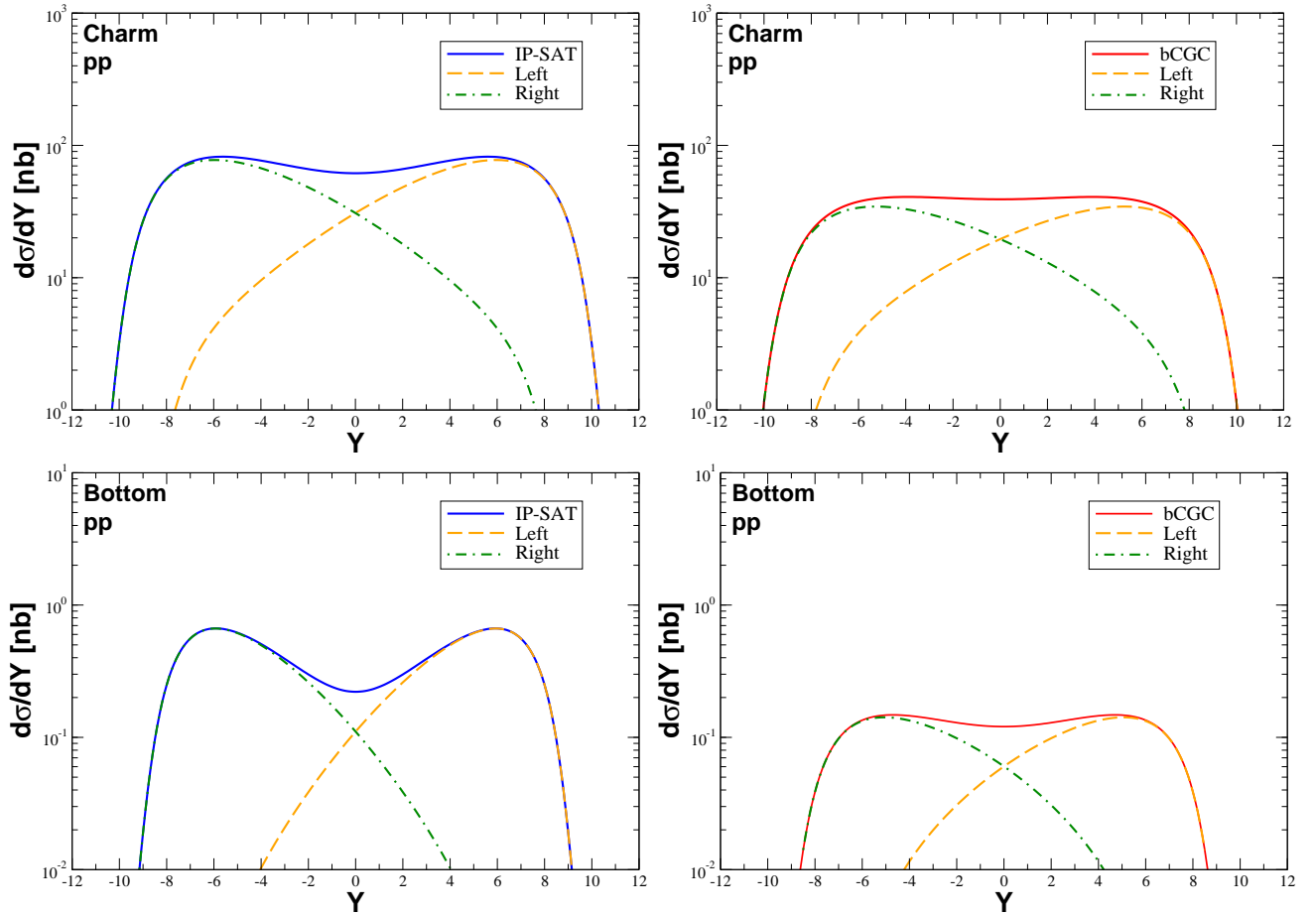


FIG. 2: Rapidity distributions for the exclusive charm (upper panels) and bottom (lower panels) photoproduction in pp collisions at the FCC ($\sqrt{s} = 100$ TeV).

with the energy than the bCGC one, which implies that the sum of the “Left” and “Right” contributions have a smaller value for central rapidity than for forward rapidities. Such behaviour is not present in the bCGC result due to the milder increasing with rapidity predicted by this model. For the charm production, the IP-SAT and bCGC predictions for the energy dependence of $\sigma_{\gamma p \rightarrow c\bar{c}p}$ are similar, implying that both models predict a plateau for central rapidities.

In Figs. 3 and 4 we present a more detailed comparison between the IP-SAT, IPnonSAT and bCGC predictions for the charm (upper panels) and bottom (lower panels) photoproduction in $pp/pPb/PbPb$ collisions at the LHC and FCC energies, respectively. Some comments are in order. For pPb and $PbPb$ collisions, the Z^2 factor, present in the nuclear photon flux, implies that the distributions are larger. For pPb collisions, we have that the distribution receives contributions of photon – proton and photon – nucleus interactions, with the photon – proton contribution being larger. It implies that the rapidity distribution is asymmetric. Moreover, in this case, the behaviour of the distribution is determined by γp interactions and the rapidity directly determines the value of x that is being probed: $x = 2m_Q e^{-Y}/\sqrt{s}$. For heavy quark production, the cross sections are dominated by the interaction of dipoles of size $r \approx 1/m_Q$ (See e.g. Ref. [32]), i.e. the charm production is dominated by larger dipole sizes than for the bottom case. As the impact of the nonlinear effects increases with the size of the dipole, we expect a larger contribution of the nonlinear effects in the case of charm production. Moreover, for the larger photon-hadron center-of-mass energies achieved at the FCC in comparison to the LHC, we also expect a larger contribution of the nonlinear effects since the impact of these effects increases at smaller values of x . Such expectations are confirmed in the results presented in Figs. 3 and 4. We have that the difference between the IP-SAT and IPnonSAT predictions is negligible for bottom production, large for charm production and increases with the energy. One can also observe a large difference between the IP-SAT and bCGC predictions, which is directly related to distinct descriptions of the linear and nonlinear regimes, as well as for the transition between these regimes. In particular, the large difference observed in the predictions for the bottom production in pp collisions is explained by the distinct treatments of the linear regime, which is dominated

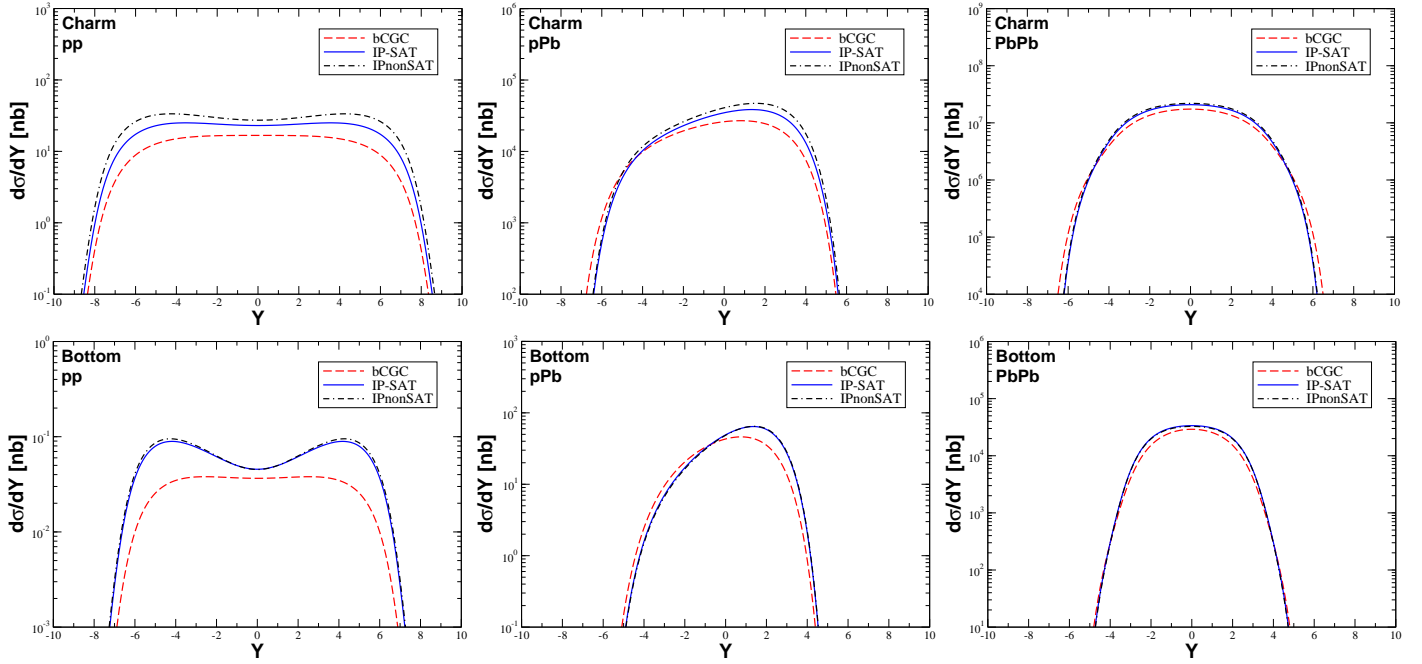


FIG. 3: Rapidity distributions for the exclusive charm (upper panels) and bottom (lower panels) photoproduction in pp ($\sqrt{s} = 13$ TeV), pPb ($\sqrt{s} = 8.1$ TeV) and $PbPb$ ($\sqrt{s} = 5.02$ TeV) collisions at the LHC.

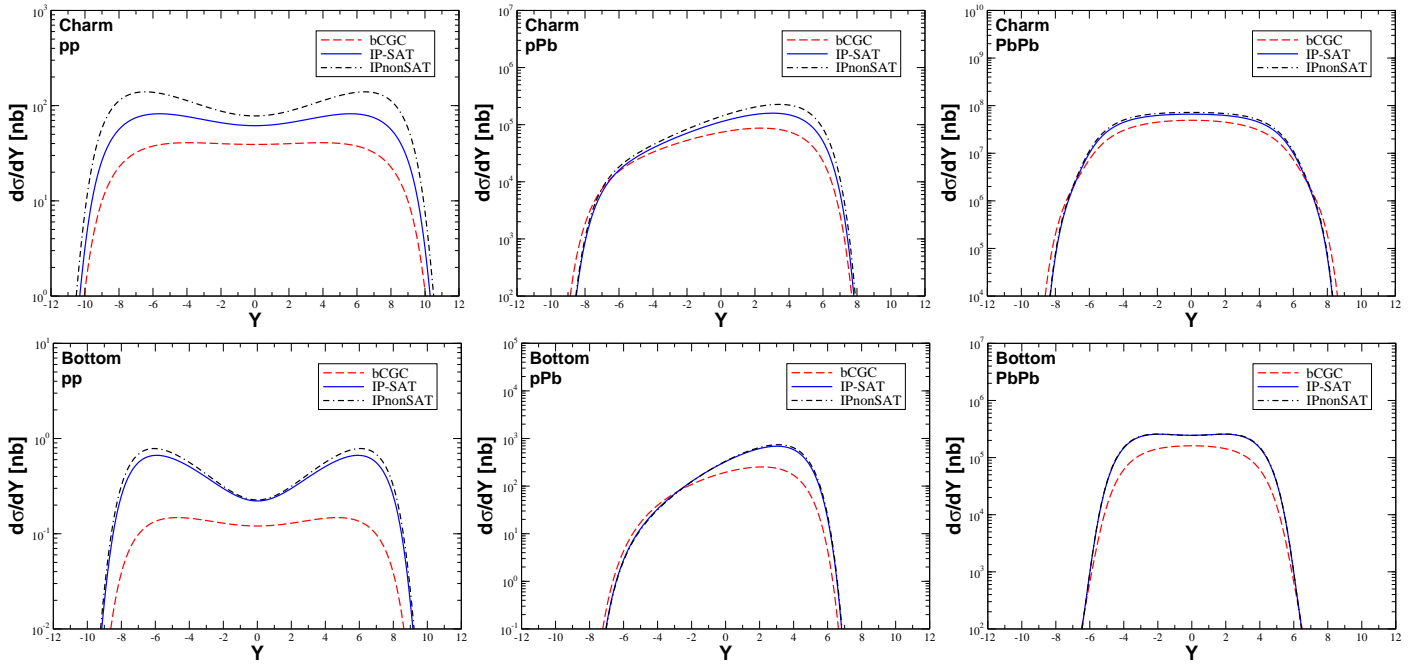


FIG. 4: Rapidity distributions for the exclusive charm (upper panels) and bottom (lower panels) photoproduction in pp ($\sqrt{s} = 100$ TeV), pPb ($\sqrt{s} = 63$ TeV) and $PbPb$ ($\sqrt{s} = 39$ TeV) collisions at the FCC.

by the interaction of very small dipoles ($r \approx 1/m_b$) with the proton. Another way to observe these distinct treatments of the linear and nonlinear regimes present in the phenomenological models is the analysis of the results for the charm production in pPb collisions. As pointed above, in this case the behaviour of the rapidity distribution is directly associated to the value that is being probed in the scattering amplitude. Therefore, for negative (positive) values of rapidity we are probing N_p at large (small)- x . One has that bCGC prediction is larger than the IP-SAT one in the linear regime and smaller in the saturation regime. For $PbPb$ collisions, this difference is smaller, which is directly

	Rapidity range	bCGC	IP-SAT	IPnonSAT
pp ($\sqrt{s} = 13$ TeV)	$-2.5 < Y < 2.5$	83.2 nb	117.9 nb	142.7 nb
	$2 < Y < 4.5$	39.3 nb	61.9 nb	80.2 nb
pp ($\sqrt{s} = 100$ TeV)	$-2.5 < Y < 2.5$	197.6 nb	320.0 nb	415.0 nb
	$2 < Y < 4.5$	101.2 nb	181.6 nb	257.1 nb
pPb ($\sqrt{s} = 8.1$ TeV)	$-2.5 < Y < 2.5$	12.0×10^4 nb	16.0×10^4 nb	19.0×10^5 nb
	$2 < Y < 4.5$	3.7×10^4 nb	6.0×10^4 nb	7.7×10^4 nb
pPb ($\sqrt{s} = 63$ TeV)	$-2.5 < Y < 2.5$	3.6×10^5 nb	5.6×10^5 nb	7.1×10^5 nb
	$2 < Y < 4.5$	2.0×10^5 nb	3.8×10^5 nb	5.5×10^5 nb
PbPb ($\sqrt{s} = 5.02$ TeV)	$-2.5 < Y < 2.5$	7.7×10^7 nb	9.3×10^7 nb	9.9×10^7 nb
	$2 < Y < 4.5$	1.9×10^7 nb	2.4×10^7 nb	2.5×10^7 nb
PbPb ($\sqrt{s} = 39$ TeV)	$-2.5 < Y < 2.5$	2.3×10^8 nb	3.2×10^8 nb	3.5×10^8 nb
	$2 < Y < 4.5$	0.9×10^8 nb	1.3×10^8 nb	1.4×10^8 nb

TABLE I: Cross sections for the exclusive charm photoproduction in $pp/pPb/PbPb$ collisions at the LHC and FCC energies considering two rapidity ranges.

	Rapidity range	bCGC	IP-SAT	IPnonSAT
pp ($\sqrt{s} = 13$ TeV)	$-2.5 < Y < 2.5$	0.2 nb	0.3 nb	0.3 nb
	$2 < Y < 4.5$	0.1 nb	0.2 nb	0.2 nb
pp ($\sqrt{s} = 100$ TeV)	$-2.5 < Y < 2.5$	0.6 nb	1.3 nb	1.4 nb
	$2 < Y < 4.5$	0.4 nb	1.1 nb	1.2 nb
pPb ($\sqrt{s} = 8.1$ TeV)	$-2.5 < Y < 2.5$	176.1 nb	217.5 nb	216.5 nb
	$2 < Y < 4.5$	30.6 nb	57.2 nb	58.7 nb
pPb ($\sqrt{s} = 63$ TeV)	$-2.5 < Y < 2.5$	937.5 nb	1750.2 nb	1804.2 nb
	$2 < Y < 4.5$	527.1 nb	1572.1 nb	1696.1 nb
PbPb ($\sqrt{s} = 5.02$ TeV)	$-2.5 < Y < 2.5$	10.1×10^4 nb	13.4×10^4 nb	13.3×10^4 nb
	$2 < Y < 4.5$	1.1×10^4 nb	1.5×10^4 nb	1.4×10^4 nb
PbPb ($\sqrt{s} = 39$ TeV)	$-2.5 < Y < 2.5$	7.6×10^5 nb	12.6×10^5 nb	12.7×10^5 nb
	$2 < Y < 4.5$	2.4×10^5 nb	5.0×10^5 nb	5.1×10^5 nb

TABLE II: Cross sections for the exclusive bottom photoproduction in $pp/pPb/PbPb$ collisions at the LHC and FCC energies considering two rapidity ranges.

associated to the fact that we are using the Glauber – Gribov model [27] to describe the dipole-nucleus scattering, with the bCGC and IP-SAT only affecting the argument of the exponential. In addition, the rapidity distributions are narrower in comparison to those for pp collisions. This behaviour is associated to the fact that the Lorentz factor γ_L is smaller for a Pb beam and $R_{Pb} > R_p$. Consequently, the value of $\omega_{\max} \approx \gamma_L/R_h$, where the rapidity distribution strongly decreases, is smaller for $PbPb$ collisions in comparison to pp one.

In Tables I and II we present the corresponding predictions for the charm and bottom cross sections, respectively, considering the rapidity ranges probed by the CMS ($-2.5 \leq Y \leq +2.5$) and LHCb ($2.0 \leq Y \leq 4.5$) detectors. One has that the predictions for the LHCb range are approximately a factor ≥ 2 smaller than those for the CMS kinematical range. We predict large values for the cross sections, in particular for the charm production in $PbPb$ collisions and FCC energies. One important question is the number of events associated to these cross sections. For the typical pp collisions at the LHC, the integrated luminosity per year is expected to be $\approx 1 \text{ fb}^{-1}$, which implies that the number of events per year will be larger than $39 (0.1) \times 10^6$ for charm (bottom) production. For the high – luminosity LHC [18], these numbers will be enhanced by a factor 350. Finally, for the FCC, where the integrated luminosity per year is expected to be $\geq 1000 \text{ fb}^{-1}$, the associated number of events will be $\geq 10^9$. For $PbPb$ collisions, the expected integrated luminosities per year for the next run of the LHC and for the FCC are 3 nb^{-1} and 110 nb^{-1} , respectively. Consequently, we predict that the number of events per year associated to charm (bottom) production in these collisions will be larger than $10^7 (10^4)$. These large numbers for the event rates indicate that a future measurement of the exclusive charm and bottom photoproduction in hadronic collisions is, in principle, feasible and that the analysis of this observable can be useful to constrain the description of the QCD dynamics at high energies. Based on these large rates, we believe that the forthcoming analysis at the LHC and FCC will also allow to perform the analysis of the differential distributions needed to constrain the elliptic component of the gluon Wigner distribution.

Finally, let's compare the predictions for the charm and bottom photoproduction in inclusive and exclusive processes, derived using the IP-SAT model. In contrast to the exclusive case, in inclusive interactions one of the incident hadrons

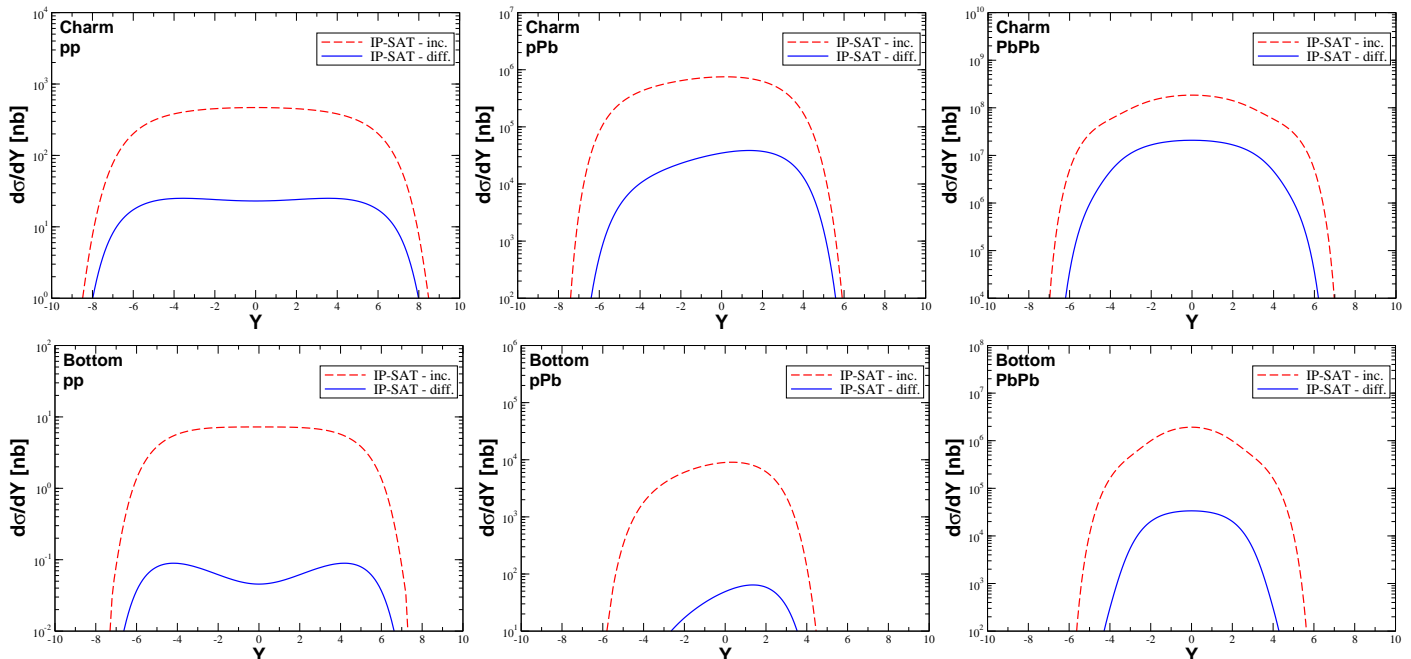


FIG. 5: Comparison between the rapidity distributions for the inclusive and exclusive charm (upper panels) and bottom (lower panels) photoproduction in pp ($\sqrt{s} = 13$ TeV), pPb ($\sqrt{s} = 8.1$ TeV) and $PbPb$ ($\sqrt{s} = 5.02$ TeV) collisions at the LHC.

fragments and the photon-hadron cross section is linearly proportional to $d\sigma/d^2\mathbf{b}_h$ (For details see, e.g. [21]). In Figs. 5 and 6 we present our results for $pp/pPb/PbPb$ collisions at the LHC and FCC energies, respectively. The results for charm (bottom) production are presented in the upper (lower) panels. In the case of charm production in pp and pPb collisions at the LHC, we have that the exclusive prediction is a factor $\mathcal{O}(20)$ smaller than the inclusive one for midrapidities. On the other hand, for $PbPb$ collisions, this factor is $\mathcal{O}(10)$. For the FCC we have that the corresponding factors are of order of 15/18/8 for $pp/pPb/PbPb$ collisions, respectively. Such results indicate that the exclusive charm production is not strongly suppressed in comparison to the inclusive case. In contrast, we have that exclusive bottom photoproduction is a factor $\mathcal{O}(100)$ [$\mathcal{O}(80)$] smaller than the inclusive one for the LHC [FCC] energies, which implies that the experimental separation of these events in the future experimental analysis will be a more difficult task. It is important to emphasize that the free parameters present in the color dipole formalism have been constrained by the HERA data, which implies that our predictions are parameter free. Moreover, as the inclusive and exclusive photoproduction in hadronic collisions are determined by the same quantities, i.e. the photon wave function and the color-dipole amplitude, a future measurement of both processes will be an important test of the universality of the color dipole formalism as well of the treatment of the nonlinear corrections to the QCD dynamics. In addition, as the Bjorken - x range probed at the FCC is beyond that probed at HERA, our predictions are based on the extrapolation of these models for a new kinematical range, where higher - order corrections can become important [33]. In principle, the magnitude of such corrections can also be constrained by the future FCC data.

IV. SUMMARY

In this paper we have computed the rapidity distributions and cross sections for the exclusive charm and bottom photoproduction in $pp/pPb/PbPb$ collisions at the LHC and FCC energies. Our study was motivated by the possibility of use this process to constrain the elliptic component of the gluon Wigner distribution by the analysis of the differential distribution in the relative quark-antiquark momentum for distinct values of the momentum transfer. Our predictions indicate that the expected number of events is very large, in particular for charm production at the FCC. Therefore, we strongly recommend a future experimental analysis of this process in order to improve our understanding of the QCD dynamics and to access the gluon Wigner distribution.

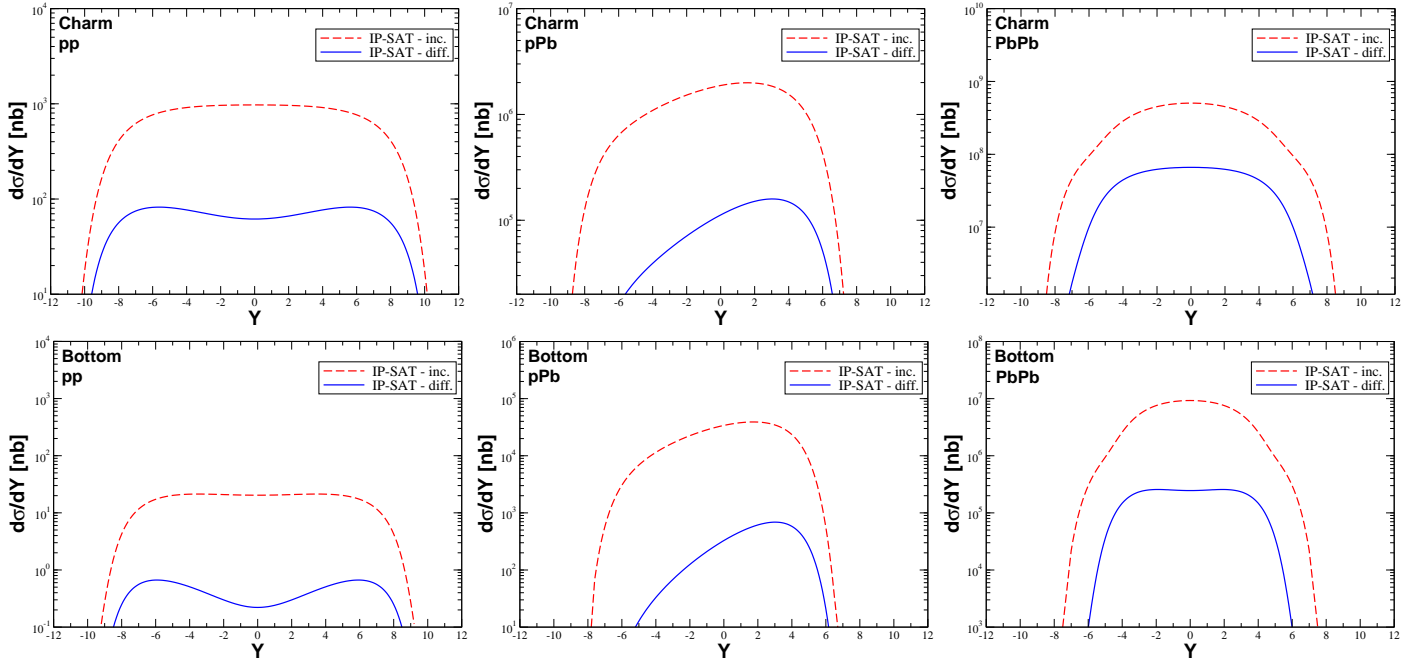


FIG. 6: Comparison between the rapidity distributions for the inclusive and exclusive charm (upper panels) and bottom (lower panels) photoproduction in pp ($\sqrt{s} = 100$ TeV), pPb ($\sqrt{s} = 63$ TeV) and $PbPb$ ($\sqrt{s} = 39$ TeV) collisions at the FCC.

Acknowledgements

VPG would like to express a special thanks to the Mainz Institute for Theoretical Physics (MITP) of the Cluster of Excellence PRISMA+ (Project ID 39083149) for its hospitality and support. This work was partially financed by the Brazilian funding agencies CAPES, CNPq, FAPERGS and INCT-FNA (process number 464898/2014-5).

-
- [1] X. d. Ji, Phys. Rev. Lett. **91**, 062001 (2003)
 - [2] M. Diehl, Phys. Rept. **388**, 41 (2003)
 - [3] A. Deshpande, R. Milner, R. Venugopalan and W. Vogelsang, Ann. Rev. Nucl. Part. Sci. **55**, 165 (2005); D. Boer, M. Diehl, R. Milner, R. Venugopalan, W. Vogelsang, D. Kaplan, H. Montgomery and S. Vigdor *et al.*, arXiv:1108.1713 [nucl-th]; A. Accardi, J. L. Albacete, M. Anselmino, N. Armesto, E. C. Aschenauer, A. Bacchetta, D. Boer and W. Brooks *et al.*, Eur. Phys. J. A **52**, no. 9, 268 (2016); E. Aschenauer, S. Fazio, J. Lee, H. Mantysaari, B. Page, B. Schenke, T. Ullrich, R. Venugopalan and P. Zurita, Rept. Prog. Phys. **82**, no.2, 024301 (2019).
 - [4] Y. Hagiwara, Y. Hatta and T. Ueda, Phys. Rev. D **94**, no. 9, 094036 (2016)
 - [5] Y. Hatta, B. W. Xiao and F. Yuan, Phys. Rev. Lett. **116**, no. 20, 202301 (2016)
 - [6] T. Altinoluk, N. Armesto, G. Beuf and A. H. Rezaeian, Phys. Lett. B **758**, 373 (2016)
 - [7] Y. Hagiwara, Y. Hatta, R. Pasechnik, M. Tasevsky and O. Teryaev, Phys. Rev. D **96**, no. 3, 034009 (2017)
 - [8] R. Boussarie, Y. Hatta, B. W. Xiao and F. Yuan, Phys. Rev. D **98**, no. 7, 074015 (2018)
 - [9] H. Mantysaari, N. Mueller and B. Schenke, Phys. Rev. D **99**, no. 7, 074004 (2019)
 - [10] F. Salazar and B. Schenke, Phys. Rev. D **100**, no. 3, 034007 (2019)
 - [11] R. Boussarie, A. V. Grabovsky, L. Szymanowski and S. Wallon, Phys. Rev. D **100**, no. 7, 074020 (2019)
 - [12] M. Reinke Pelicer, E. Grave De Oliveira and R. Pasechnik, Phys. Rev. D **99**, no. 3, 034016 (2019)
 - [13] Y. Hatta, N. Mueller, T. Ueda and F. Yuan, arXiv:1907.09491 [hep-ph].
 - [14] C. A. Bertulani and G. Baur, Phys. Rep. **163**, 299 (1988); F. Krauss, M. Greiner and G. Soff, Prog. Part. Nucl. Phys. **39**, 503 (1997); G. Baur, K. Hencken and D. Trautmann, J. Phys. G **24**, 1657 (1998); G. Baur, K. Hencken, D. Trautmann, S. Sadovsky, Y. Kharlov, Phys. Rep. **364**, 359 (2002); C. A. Bertulani, S. R. Klein and J. Nystrand, Ann. Rev. Nucl. Part. Sci. **55**, 271 (2005); V. P. Goncalves and M. V. T. Machado, J. Phys. G **32**, 295 (2006); A. J. Baltz *et al.*, Phys. Rept. **458**, 1 (2008); J. G. Contreras and J. D. Tapia Takaki, Int. J. Mod. Phys. A **30**, 1542012 (2015).
 - [15] V. P. Goncalves and M. V. T. Machado, Phys. Rev. D **75**, 031502 (2007)
 - [16] F. Gelis, E. Iancu, J. Jalilian-Marian and R. Venugopalan, Ann. Rev. Nucl. Part. Sci. **60**, 463 (2010); H. Weigert, Prog. Part. Nucl. Phys. **55**, 461 (2005); J. Jalilian-Marian and Y. V. Kovchegov, Prog. Part. Nucl. Phys. **56**, 104 (2006).

- [17] J. Jalilian-Marian, A. Kovner, L. McLerran and H. Weigert, Phys. Rev. D **55**, 5414 (1997); J. Jalilian-Marian, A. Kovner and H. Weigert, Phys. Rev. D **59**, 014014 (1999); Phys. Rev. D **59**, 014015 (1999); Phys. Rev. D **59**, 034007 (1999); E. Iancu, A. Leonidov and L. McLerran, Nucl. Phys. **A692**, 583 (2001); E. Ferreiro, E. Iancu, A. Leonidov and L. McLerran, Nucl. Phys. **A701**, 489 (2002); H. Weigert, Nucl. Phys. **A703**, 823 (2002).
- [18] A. Abada *et al.* [FCC Collaboration], Eur. Phys. J. C **79**, no. 6, 474 (2019); Eur. Phys. J. ST **228**, no. 4, 755 (2019); Eur. Phys. J. ST **228**, no. 5, 1109 (2019).
- [19] M. Drees and D. Zeppenfeld, Phys. Rev. D **39**, 2536 (1989).
- [20] N. N. Nikolaev, B. G. Zakharov, Phys. Lett. B **332**, 184 (1994); Z. Phys. C **64**, 631 (1994).
- [21] V. P. Goncalves, G. Sampaio dos Santos and C. R. Sena, Nucl. Phys. A **976**, 33 (2018)
- [22] H. Kowalski, L. Motyka and G. Watt, Phys. Rev. D **74**, 074016 (2006).
- [23] H. Kowalski and D. Teaney, Phys. Rev. D **68**, 114005 (2003).
- [24] E. Levin and K. Tuchin, Nucl. Phys. A **691**, 779 (2001)
- [25] A. H. Rezaeian and I. Schmidt, Phys. Rev. D **88**, 074016 (2013)
- [26] H. Mantysaari and P. Zurita, Phys. Rev. D **98**, 036002 (2018)
- [27] N. Armesto, Eur. Phys. J. C **26**, 35 (2002).
- [28] R. J. Glauber, in Lecture in Theoretical Physics, Vol. 1, edited by W. E. Brittin, L. G. Duham (Interscience, New York, 1959).
- [29] V. N. Gribov, Sov. Phys. JETP **29**, 483 (1969); Sov. Phys. JETP **30**, 709 (1970).
- [30] A. H. Mueller, Nucl. Phys. B **335**, 115 (1990).
- [31] E. R. Cazaroto, F. Carvalho, V. P. Goncalves and F. S. Navarra, Phys. Lett. B **671**, 233 (2009)
- [32] M. S. Kugeratski, V. P. Goncalves and F. S. Navarra, Eur. Phys. J. C **46**, 465 (2006); Eur. Phys. J. C **46**, 413 (2006)
- [33] T. Lappi and H. Mantysaari, Phys. Rev. D **91**, no.7, 074016 (2015); Phys. Rev. D **93**, no.9, 094004 (2016); B. Ducloue, H. Hanninen, T. Lappi and Y. Zhu, Phys. Rev. D **96**, no.9, 094017 (2017)